Calibration of a Candidate GIFTS/GLOBE Water Vapor Sun Photometer by Intercomparison with Microwave Observations During the 2000 Water Vapor IOP

L. A. Sromovsky, S. S. Limaye, P. M. Fry, R. O. Knuteson, B. Osborne,
H. E. Revercomb, R. Tamanachi, and D. C. Tobin
Space Science and Engineering Center
University of Wisconsin-Madison
Madison, Wisconsin

Introduction

As a component of the National Aeronautics and Space Administration (NASA) New Millennium Program Geostationary Imaging FTS (GIFTS) mission, we are developing an Education and Public Outreach (EPO) program. As part of this EPO effort, measurement of precipitable water vapor from schools will be made in collaboration with the Global Learning and Observations to Benefit the Environment (GLOBE) program. Current plans are to use an inexpensive sun photometer with two light emitting diodes (LEDs) employed as narrow-band detectors. By measuring solar irradiance at two nearby wavelengths sampling different degrees of water vapor absorption, students will be able to make an approximate determination of total precipitable water vapor. A candidate instrument of this type was operated at the Oklahoma Cloud and Radiation Testbed (CART) site during the 2000 Water Vapor Intensive Operational Period (IOP) to permit comparison with Microwave Radiometer (MWR) and Ames Airborne Tracking Sunphotometer (AATS) observation. The intercomparison provides validation of the basic approach and calibration of the instrument.

GIFTS-GLOBE Sun Photometer

The preliminary GIFTS-GLOBE photometer design is based on the work of Forest Mims III (1992), who pioneered the use of LEDs as narrow-band radiation detectors, and on the GLOBE haze photometer (Mims 1999). In these sun photometers, LEDs serve as inexpensive "monochromatic" detectors without the need for narrow-band filters. For about $25 in component costs, the GLOBE photometers can be built by middle school and high school students as part of a technology education process. As illustrated in Figure 1, the candidate GIFTS version of the photometer has two LEDs, with emission wavelengths of 880 and 940 nm, two op-amps to convert photo current to voltage, a small circuit board, a 9 V battery, a small plastic case equipped with two apertures for admitting solar beam radiation, and an external sight to facilitate accurate pointing. The angular field of view is about 2° full width at half maximum. We added a thermistor to the GIFTS photometer to investigate corrections for temperature dependence in the LED spectral response, which turned out to have significant effects on the derived precipitable water vapor. While the haze sensing version of the sun photometer can be calibrated by the Langley
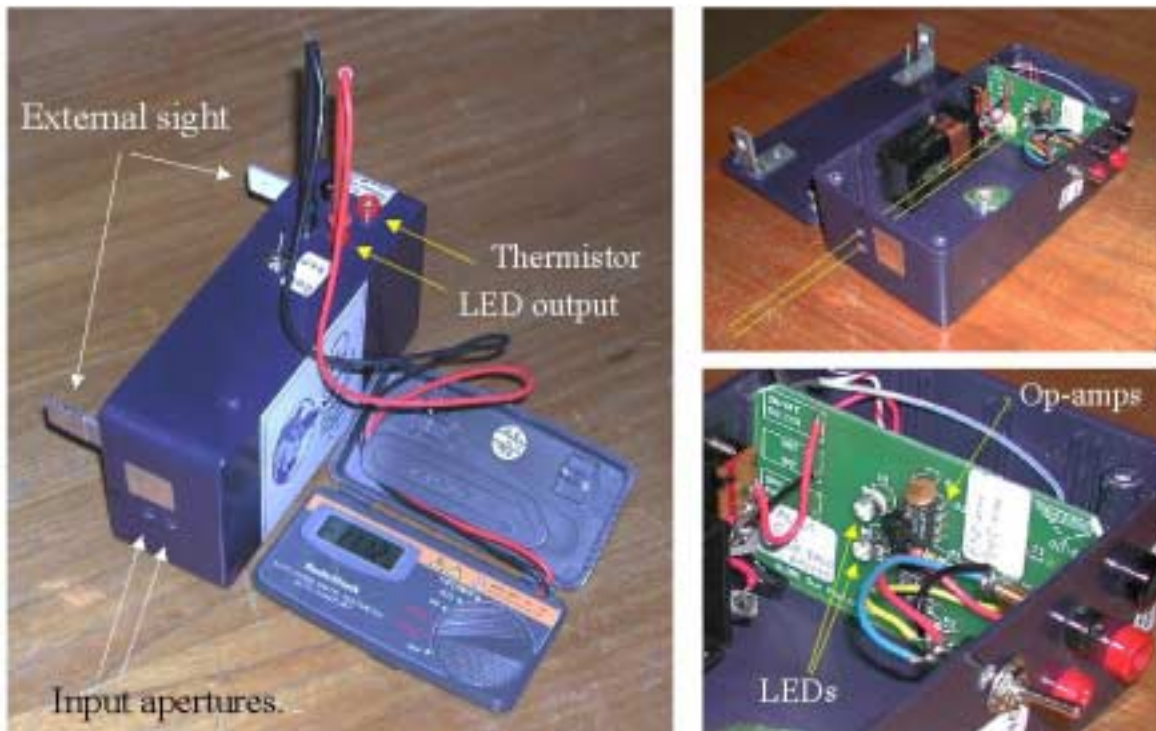
Figure 1. Preliminary version of the GIFTS-GLOBE sun photometer. Two LEDs, with peak sensitivities at 817.7 and 915 nm, are mounted on a small circuit board with op-amps that convert photo current to voltage, and a thermistor to sense LED temperature. Input apertures permit solar beam radiation to fall on the LEDs when an external sight is aimed at the sun. An inexpensive multi-meter is used to read out voltages and thermistor resistance. The plastic case is about 6 inches long.

method, the complexity of modeling water vapor absorption and the frequently large temporal variability of water vapor make intercomparisons with simultaneous independent measurements a preferred calibration approach.

Measurement Concept

The use of solar transmission measurements in and out of the 940-nm water vapor absorption band is a well established method for measuring precipitable water (Thome et al. 1992, 1994; Reagan et al. 1995; Schmid et al. 1996). We follow these references in modeling atmospheric transmission in the water vapor bands as $\ln (T) = a + b \, (mu)^{1/2}$, where m is air mass (1/sin[elevation angle]) and u is column water vapor amount (usually measured in precipitable centimeter). The band model refers to an equivalent absorber amount, which here we take to be the actual amount. We assume that the difference between these two measures can be incorporated into the two empirically determined constants (a and b), so long as the vertical distribution of water and the atmospheric temperature structure is relatively invariant. More extensive comparisons will be needed to correct for such variations.

Because the LED detection peaks are wavelength shifted relative to their emission peaks (817.5 nm versus 880 nm, and 915 nm versus 940 nm), the chosen LEDs are not ideally positioned with respect to the water vapor absorption features (see Figure 2). These shifts and the wings of the response functions result in both of our detector channels being affected by some degree of water vapor absorption, the 880 nm LED affected more than intended and the 940-nm LED affected less than intended. We use a similar transmission model for both bands, but with different constants. Our model for the ratio of voltage measurements for the two detectors then becomes

$$\ln(V_{880}/V_{940}) = \ln K - m \, \delta\tau_R - m \, \delta\tau_A - (b_{880}-b_{940}) \, (mu)^{1/2} , \tag{1}$$

where m is air mass, $\delta\tau_R$ is the difference in Rayleigh optical depths at 817.5 nm and 915 nm, $\delta\tau_A$ is the difference in aerosol optical depths between the two wavelengths, and K is a constant that depends on the difference in offsets ($a_{880}-a_{940}$), the ratio of solar fluxes at the two wavelengths, the ratio of detector and preamp gains, and ratio of spectral bandwidths. In the following, we ignore differential Rayleigh and aerosol contributions, which are both estimated to be less than 0.01 per air mass for the observations in question.

Observations During the Water Vapor IOP

We obtained GIFTS-GLOBE photometer observations over the September 16 to October 3, 2000, time period. The data best suited for intercomparison were gathered during September 18 to 22 when large variations in column water vapor (CWV) occurred and when we also had good coincident MWR observations. We removed spikes from the MWR data before to interpolation to the times of the photometer observations. The photometer voltage ratios vary because of varying air mass as well as due to variations in CWV. Air mass values ranged from 1.2 to 15, CWV from 1 to 4.3 precipitable centimeter, and photometer temperatures from 21° to 36° Celsius. For most observations, aerosol optical depths at 864 nm were between 0.05 and 0.25.

Modeling CWV Dependence Using MWR Observations

Using the previously described model for atmospheric transmission, we plotted the square root of the MWR column water vapor-air mass product as a function of the log of the photometer voltage ratio. The resulting nearly linear dependence is partial confirmation of the assumed model. We used two different linear model equations:

$$(u \, m)^{1/2} = C + D \log_e (V_{940}/V_{880}), \text{ and } (u \, m \, f(T))^{1/2} = C + D \log_e (V_{940}/V_{880}), \tag{2}$$

where the first ignores temperature corrections, and the second incorporates a temperature correction factor f(T) derived in the next section. Least squares linear regression fits yielded constant values of C = -3.21±0.26 and D = -8.5± 0.4 with $\chi^2 = 1.11$ for the first model and C = -3.35±0.24 and D = -8.8±0.4 with $\chi^2 = 0.94$ for the second model, which includes temperature corrections. The latter model provides only a marginal improvement for this data set, but is very important for later data taken
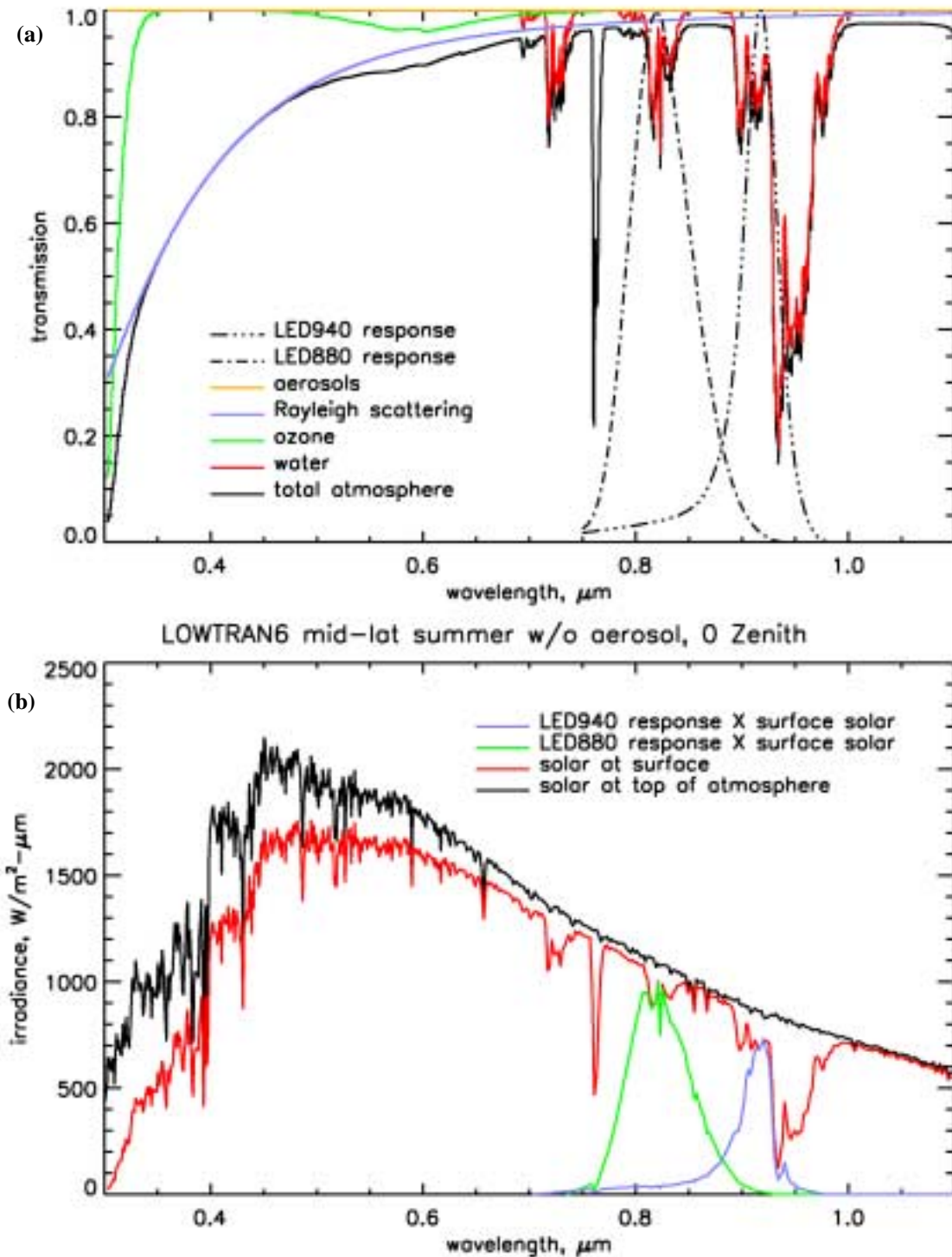
Figure 2. (a) Atmospheric transmission spectrum for a mid-latitude summer atmosphere without aerosols, with separately displayed contributions from Rayleigh scattering, ozone, and water vapor, compared to relative spectral responses of LEDs with emission peaks at 880 and 940 nm.
(b) Corresponding irradiance spectra and LED response times the solar spectral irradiance at the surface.

during large variations in LED temperatures (see next section). From these fits we obtain equations for computing precipitable water, which can be written as

$$u = G \ (\log_e (KV_{940}/V_{880}))^2/(m \ f(T)), \text{ where } G = D^2 \text{ and } K = e^{C/D}. \tag{3}$$

Figure 3a compares the best-fit model CWV values to the MWR results that were used to determine the model coefficients, both with and without temperature corrections. The agreement is generally within 10% to 20%. Figure 3b displays the temperature correction curve that we inferred from comparisons with CWV amounts determined from the AATS observations, which are discussed in the following section.

Comparison with AATS Observations

Using the calibration obtained above from the MWR observations, we computed GIFTS-GLOBE photometer estimates for column water vapor for the period through September 30, 2000. These are compared with AATS observations in Figure 4. On September 29, the AATS results indicate low and constant CWV (red curve) and very low aerosol amounts (cyan curve). The GIFTS-GLOBE variations during that period exhibit factor-of-two variations in derived water amounts that are very well correlated with the temperature of the LED circuit board (shown in Figure 3b). Using a simple quadratic fit to the GIFTS/AATS ratio, we obtained a correction function that approximately accounts for variations in LED response with temperature. When applied to the observations, the GIFTS-GLOBE results provide excellent agreement with both MWR and AATS, provided that we scale the AATS by a factor of 1.1.

The temperature dependence of the GIFTS-GLOBE photometer arises primarily from the wavelength shift of the LED spectral response function. As the LED temperature increases, its peak response moves to longer wavelengths, at a rate of about 7 nm per 20° Celsius. This moves the longwave LED into the more strongly absorbing part of the 940 nm H_2O band, which produces an increase in the derived CWV amount, if uncorrected.

Conclusions

The two-channel LED GIFTS-GLOBE sun photometer can provide useful estimates of column water vapor amounts from a simple voltage ratio measurement. The model that relates the voltage ratio to CWV can be calibrated by comparisons to MWR observations over a range of CWV values. Temperature corrections are needed with the existing LED detectors, but a simple correction equation, based on thermistor measurements of LED temperatures, appears to be relatively effective. A wider variety of intercomparisons is needed to determine variations associated with seasonal differences in water vapor distributions and temperature structure. We are evaluating additional LEDs, with the aim of finding peak wavelengths and bandwidths that optimize sensitivity to water vapor at high elevation angles and minimize sensitivity to temperature.
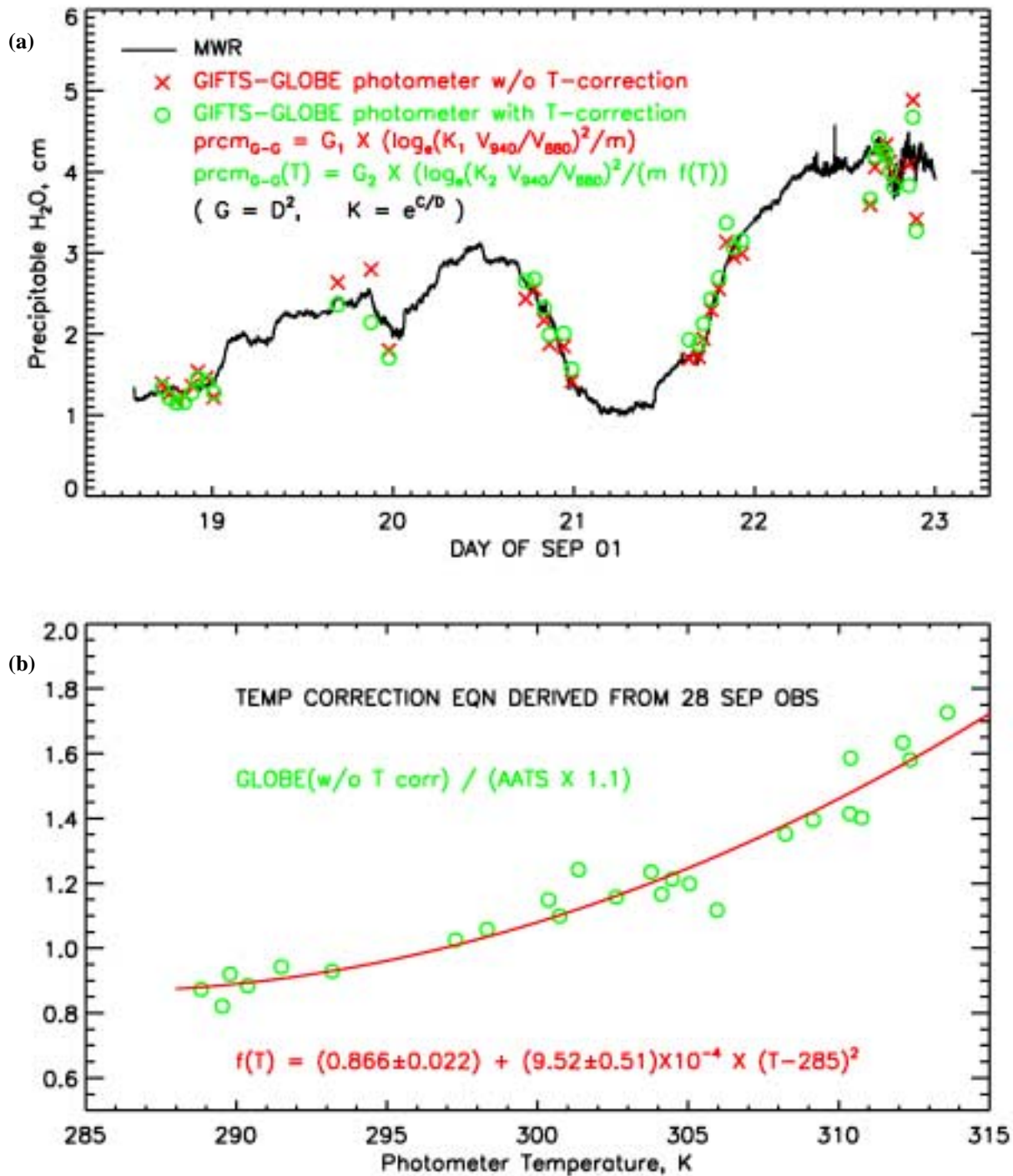
Figure 3. (a) Comparison of MWR – derived precipitable water vapor (black) with the best fit empirical results from the GIFTS-GLOBE photometer observations without using temperature corrections (red) and with temperature corrections (green). (b) Observed ratios (green circles) of GIFTS-GLOBE precipitable water without temperature corrections to 1.1 times the AATS results, displayed as a function of photometer circuit board temperature, compared to a quadratic fit used for temperature correction.
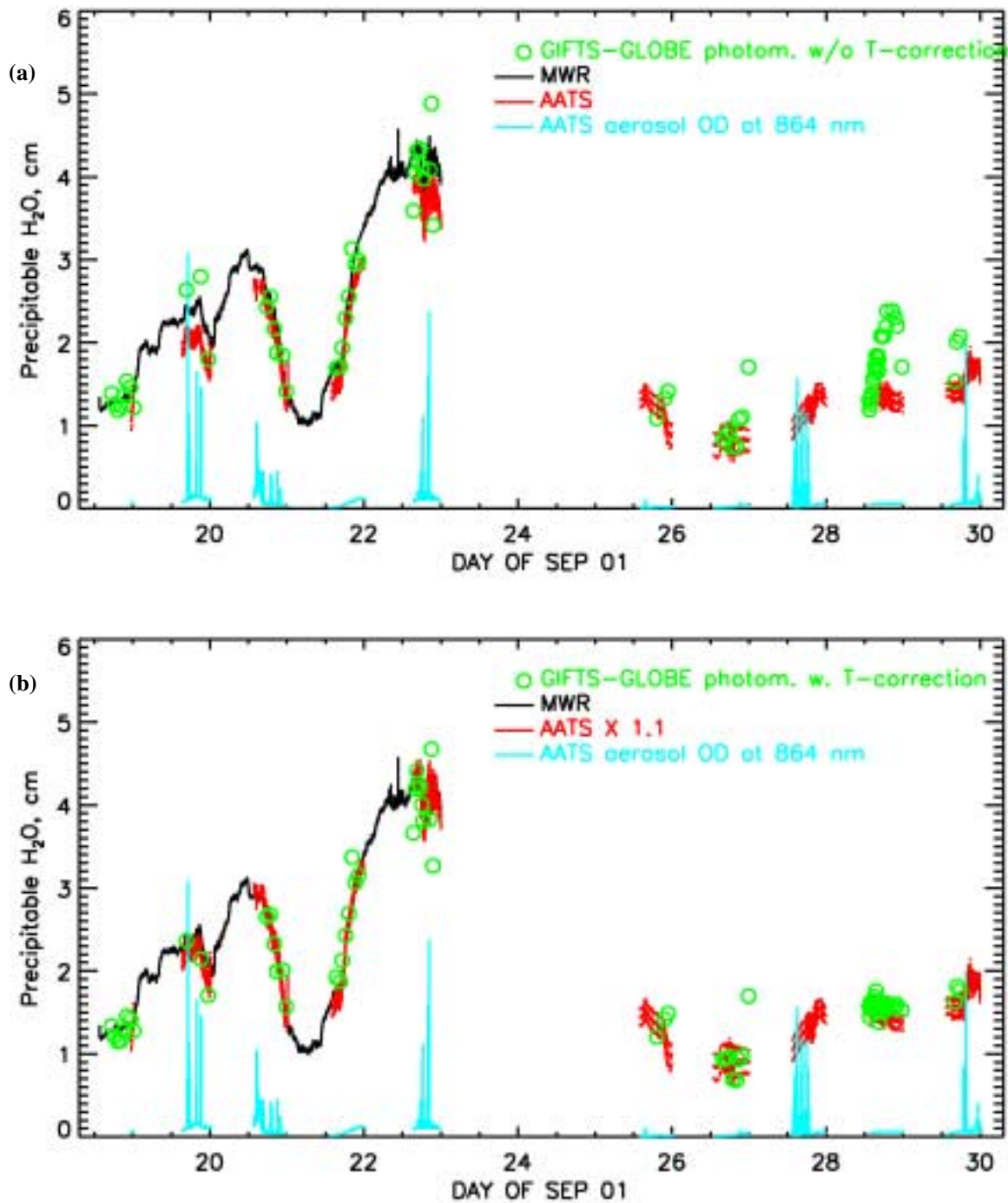
Figure 4. (a) Comparison of the empirical fit of the GIFTS-GLOBE photometer results (green circles) with the precipitable water vapor obtained from the AATS (red). The large discrepancy during September 28 is due to variations in the temperature of the GIFTS-GLOBE photometer (see Figure 3). The AATS aerosol optical depth at 864 nm is shown by the cyan curve. (b) As in the upper panel, except that the empirical GIFTS-GLOBE fit incorporates the temperature dependence given in Figure 3, and the AATS precipitable water values are multiplied by 1.1 to achieve consistency with the MWR results.

Corresponding Author

L. A. Sromovsky, larry.sromovsky@ssec.wisc.edu, (608) 263-6785

References

Mims, F. M. III, 1992: Sun photometer with light-emitting diodes as spectrally selective detectors. *Appl. Opt.*, **31**, 6965-6967.

Mims, F. M. III, 1999: An international haze monitoring network for students. *Bull. Am. Met. Soc.*, **80**, 1421-1431.

Thome, K. J ., B. M. Herman, and J. A. Reagan, 1992: Determination of precipitable water from solar transmission. *J. Appl. Met.*, **31**, 157-165.

Thome, K. J., M. W. Smith, J. M. Palmer, and J. A. Reagan, 1994: Three-channel solar radiometer for the determination of atmospheric columnar water vapor. *Appl. Opt.*, **33**, 5811-5819.

Reagan, J., K. Thome, B. Herman, R. Stone, J. DeLuisi, and J. Snider, 1995: A comparison of columnar water vapor retrievals obtained with near-IR solar radiometer and microwave radiometer measurements. *J. Appl. Met.*, **34**.

Schmid B., K. J. Thome, P. Demoulin, R. Peter, C. Matzler, and J. Sekler, 1996: Comparison of modeled and empirical approaches for retrieving columnar water vapor from solar transmittance measurements in the 0.94-micron region. *J. Geophys. Res.*, **101**, 9345-9358.